

Absolute distance measurement system using a femtosecond laser as a modulator

This article has been downloaded from IOPscience. Please scroll down to see the full text article.

2010 Meas. Sci. Technol. 21 115302

(<http://iopscience.iop.org/0957-0233/21/11/115302>)

View [the table of contents for this issue](#), or go to the [journal homepage](#) for more

Download details:

IP Address: 128.103.149.52

The article was downloaded on 07/03/2011 at 17:51

Please note that [terms and conditions apply](#).

Absolute distance measurement system using a femtosecond laser as a modulator

Nicolae R Doloca, Karl Meiners-Hagen, Martin Wedde, Florian Pollinger and Ahmed Abou-Zeid

Physikalisch-Technische Bundesanstalt, Bundesallee 100, D-38116 Braunschweig, Germany

E-mail: nicolae.r.doloca@ptb.de

Received 27 May 2010, in final form 22 July 2010

Published 24 September 2010

Online at stacks.iop.org/MST/21/115302

Abstract

The generation of broadband microwave frequency comb from a femtosecond pulse train by direct photodetection opens the possibility for high-accuracy length measurements of long distances. We demonstrate a relatively simple realization of this measurement principle: an electronic distance measurement system based on a time-of-flight approach, driven by a femtosecond fibre laser source as a modulator. By the evaluation of the phase shifts of two distinct comb frequencies, a coarse and a fine measurement of the absolute distance can be performed. The range of the measurement system is demonstrated up to a length of 100 m. The experimental comparison of the femtosecond laser system with a conventional reference counting interferometer shows a precision better than $\pm 10 \mu\text{m}$ at 100 m, corresponding to a relative measurement uncertainty of $1 \times 10^{-7} L$. The limiting factors for the measurement uncertainty of the system are theoretically investigated and shown to be of the same order of magnitude.

Keywords: absolute distance measurement, femtosecond laser, time-of-flight

1. Introduction

High-precision measurements of long distances have recently drawn increased attention [1, 2]. Growing demands in large-scale production or global monitoring require a higher level of accuracy below 10^{-6} for measurement and quality tests over long-range distances (above 10 metres up to several kilometres). In particular, devices of sufficient accuracy to establish a traceability chain for GPS-based distance measurements are missing from the metrological point of view. In principle, optical interferometry is the classical tool for distance measurements in industrial application or for calibration of precision machines with a measurement uncertainty which is far better than the wavelength of the used light. Indisputably, however, the main disadvantage of classical interferometry for its application for long distances is the fact that only incremental measurements are possible. Therefore, interferometry-based length measurements require either a continuously delayed movement or complementary input on the length with sufficient accuracy, e.g. by multi-wavelength interferometry [3–6]. Currently, long-range measurements are mainly performed by instruments based on electronic distance measurement (EDM). Relative accuracies down to approximately 10^{-6} can be achieved without

mechanical guidance, and the overall effort is limited. EDMs are usually based on optoelectronic phase-shifting methods, the distance probed by amplitude-modulated laser beams. Compared with interferometric techniques, their accuracy is lower, but unambiguous measurements over larger distances, namely the half period length of the modulated beam, are possible. Generally speaking, the measurement resolution decreases with larger unambiguity ranges.

Driven by advances in technology, femtosecond (fs) laser sources have become an interesting tool for distance measurements in the last decade [1]. When referenced to the signal of atomic clocks, length measurements performed by fs-frequency combs can be directly traced back to the SI definition of the metre. Furthermore, the large range of unambiguity length in the metre regime, determined by frequency mode spacing and thus ultimately by the resonator length, makes them particularly interesting for long-distance measurements. Moreover, the fs laser can be applied both in interferometric and in EDM-based systems. By using a fs laser as source in a suitable combination of these methods, incremental procedures can be avoided. The pioneering work of Minoshima and Matsumoto [7] demonstrated the first fs-based EDM system. Meanwhile, also interferometric

approaches for absolute length measurements have been realized [8, 9]. Ye [10] proposed for the first time a phase-stabilized fs pulse train for time-of-flight detection with transition to fringe-resolved measurement of coherent cross-correlation between fs pulses. Measurements based on cross-correlation function analysis [11] showed a relative uncertainty of about 3×10^{-8} .

Although interferometric approaches make uncertainties in the sub-wavelength regime possible, the realization of the cross-correlation condition requires moving reference arms, leading to long measurement times. Furthermore, hybrid solutions that combine the advantages of time-of-flight and interferometric approaches, such as described in [12], are extremely complex systems requiring the use of two-frequency comb sources.

This paper describes a time-of-flight-based approach, using a fs-frequency comb as a modulator. The unambiguity on metre and centimetre scales was achieved by phase analysis of different microwave frequency lines generated during the detection of the fs laser pulses with a high-speed photodiode. Our approach uses a harmonic frequency line of 11.4 GHz for the high-resolution distance measurement. Thereby, a relative uncertainty of 1×10^{-7} was achieved on measurement distances of up to 100 m under laboratory conditions. Finally, the factors limiting the measurement uncertainty of our system were investigated in detail.

2. Measurement principle: the fs laser as an EDM modulator

The measurement principle is relatively straightforward, as previously demonstrated by the works of Minoshima's group [7, 13–15]. A fs pulse train generated by a fs-frequency comb is split and traverses a fixed reference and a measurement path. Both signals are then detected by high-speed photodiodes. The spectrum generated by the photodiode contains harmonics of the pulse repetition frequency f_{rep} (in our case 100 MHz), up to the nominal bandwidth limit of the photodiode in the microwave regime. The resulting 'generic' frequency comb in the microwave range is depicted in figure 1. Any change in the optical path length of the laser beam induces continuous phase shifts at each frequency line also in this microwave comb. Therefore, direct information about the absolute path length of the beam can be deduced by a combined phase analysis of two frequency lines. However, the most important condition for the realization of such a measurement principle is very high stability of the pulse repetition rate.

For the correct interpretation of the phase shifts, one has to take into account that the propagation of the laser pulses is determined in air due to dispersion by the group refractive index n_g . Due to the fact that air is a low dispersive propagation medium, and also it presents no absorption line in the proximity of our laser beam wavelength $\lambda = 780$ nm, the wave group travels considerable distance without appreciable diffusion or absorption. Under these circumstances the group refractive index can be expressed in the form [16, 17]

$$n_g = n - \lambda \frac{\partial n}{\partial \lambda}, \quad (1)$$

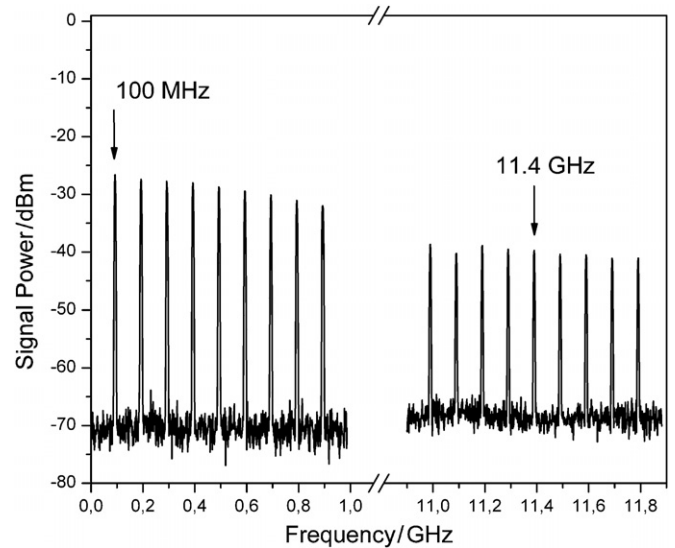


Figure 1. Experimental frequency comb spectrum of the photodiode signals. The peaks at 100 MHz and 11.4 GHz are the two frequency lines analysed in the experiment for the length measurement.

n being the phase refractive index. It can be deduced from the ambient conditions temperature T , pressure p and relative humidity by using the empirical formula of Bönsch and Potulski [18].

The measurement process consists of two steps. In the first step, the length is finely determined by the acquisition of the high-frequency line at $f_1 = 11.4$ GHz. Due to the modulo 2π phase determination, the phase value Φ_1 of the signal f_1 provides length information l_1 within the unambiguous range $\Lambda_1 \approx 13$ mm:

$$l_1 = \frac{\Phi_1}{2\pi} \frac{c}{2f_1 n_g} = \frac{\Phi_1}{2\pi} \Lambda_1, \quad (2)$$

with c being the speed of light in vacuum and n_g being the group refractive index in air for the laser beam wavelength λ of 780 nm. To unwrap the phase result of the fine measurement, a coarse determination in a second step is necessary. For this purpose, the phase Φ_2 of the first frequency line at $f_2 = f_{\text{rep}} = 100$ MHz is analysed, resulting in a length information l_2 within the unambiguous range of $\Lambda_2 = 1.5$ m:

$$l_2 = \frac{\Phi_2}{2\pi} \frac{c}{2f_{\text{rep}} n_g} = \frac{\Phi_2}{2\pi} \Lambda_2. \quad (3)$$

The measurement uncertainty of the second detection must be lower than half of the unambiguous range of the first step to obtain the right integer order N_1 of the fine measurement with 11.4 GHz [5].

If the target is located at a distance previously known with an uncertainty better than Λ_2 , e.g. by conventional EDM techniques, the absolute length can be reconstructed. If this is not the case, a third step is necessary in order to unwrap the coarse measurement of Λ_2 period. For this purpose, the pulse repetition rate can be slightly changed to $f'_{\text{rep}} = 100.1$ MHz, and the resulting phase shift of the first comb line can be converted into a coarse length determination within an unambiguous range of $\Lambda_3 \approx 1.5$ km:

$$\Lambda_3 = \frac{c}{2(f'_{\text{rep}} - f_{\text{rep}}) n_g}. \quad (4)$$

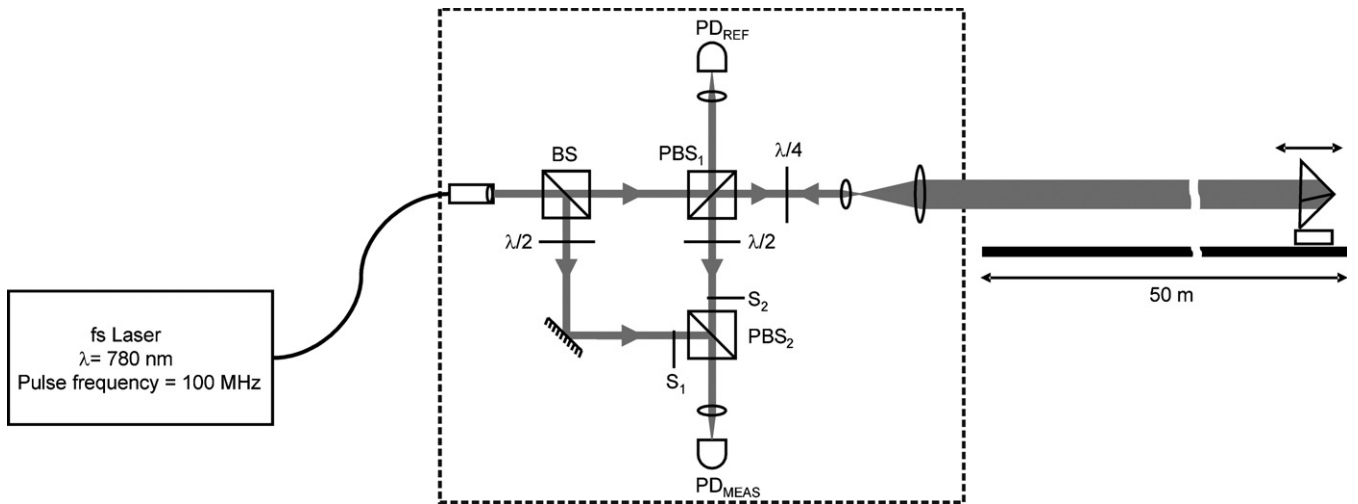


Figure 2. The optical setup of the fs distance measurement system.

Similar to the previous step, the measurement uncertainty of this step must be smaller than half of the unambiguous range Λ_2 in order to determine the integer order N_2 of the measurement with 100 MHz. By combining all three steps and applying the mathematical analysis described in [5], the absolute length can be finally expressed as follows:

$$l = \text{floor} \left[\frac{N_2 \Lambda_2 + \frac{\Phi_2}{2\pi} \Lambda_2}{\Lambda_1} - \frac{\Phi_1}{2\pi} + \frac{1}{2} \right] \Lambda_1 + \frac{\Phi_1}{2\pi} \Lambda_1. \quad (5)$$

3. Experimental set-up

A stabilized mode-locked erbium femtosecond fibre laser of wavelength $\lambda = 780$ nm (Menlo Systems C-Fiber 780 Sync) was used providing pulses of 100 fs width with a repetition rate f_{rep} of 100 MHz. To ensure the necessary high stability of the intermode beat frequencies, the laser system is equipped with a repetition rate stabilizer module. The optical part of the system is schematically shown in figure 2. By using the polarizing beam splitter PBS_1 , the reflected part is focused onto the high-speed photodiode PD_{REF} (New Focus Model 1437). There, the reference signal is generated in the form of electric signals of frequency comb lines up to 25 GHz, the frequency limit of the detector. The transmitted part, which is used as the measurement beam, is expanded, collimated and further directed onto the triple-mirror retroreflector target. The back reflected laser pulses re-enter the collimation system. After twice 90° rotation of the polarization by a quarter-waveplate, the measurement beam is reflected by the splitter PBS_1 and focused onto the second high-speed photodiode PD_{MEAS} , on which the measurement frequency comb is generated.

The electronic design of the system is depicted in figure 3. First, the high-frequency (HF) spectrum of the comb is separated from the low-frequency (LF) range. To avoid loss in signal power, two custom-made HF diplexers are used to separate comb lines above 500 MHz from the first five low-frequency lines. In order to obtain the phase information of the fine measurement, a frequency-mixing procedure is

followed. The comb line at f_1 is mixed with a signal of slightly different frequency ($\Delta f = 25$ kHz) generated by a local oscillator (Rohde & Schwartz SMF100A). Thus, intermediary beat frequency signals in the kHz range, IF_{MEAS} and IF_{REF} , are obtained on both measurement and reference arms. The two beat frequency signals are amplified and further transmitted to a lock-in amplifier deducing the phase difference between measurement and reference signals.

The experimental set-up is similar to the system described in [13–15]. The difference consists in the mixing type of the intermode beats. Our approach uses an external local oscillator, while Minoshima's system mixes first the frequency mode of interest $f_{\text{IM}} = 10$ GHz of the measurement signal with the adjacent frequency mode $f_{\text{IM}} - f_{\text{Mrep}}$ of the reference signal. The phase of the resulting intermediary frequency $f_{\text{Mrep}} = 50$ kHz is analysed in relation to the intermode beat at f_{Mrep} of the reference signal.

High-frequency electronics is very sensitive to even small change in temperature, inducing length variations in the high-frequency cables, resulting in phase measurement errors. In order to compensate such effects, an additional compensation length is measured, as shown in figure 2. A part of the laser beam is reflected at the beam splitters, BS and PBS_2 , and directly focussed onto the photodiode PD_{MEAS} , without traversing the measurement path. The resulting signal corresponds to a length measurement for a very short, but constant distance. Using two mechanical shutters S_1 and S_2 , the measurement and the compensation path beams are sequentially focused on PD_{MEAS} . The same correction scheme was also applied in [14, 15]. Since the detection errors caused by the electronics influence measurement and compensation signals in the same way, electronic drift effects slower than the total measurement time of 6 s are cancelled out by considering the phase difference between both signals. As a consequence, the long-time stability of the measurement improves significantly, as shown in figure 4, for 1 hour period of measurement time.

Working at lower frequencies, a slightly different detection scheme can be applied for the coarse measurement.

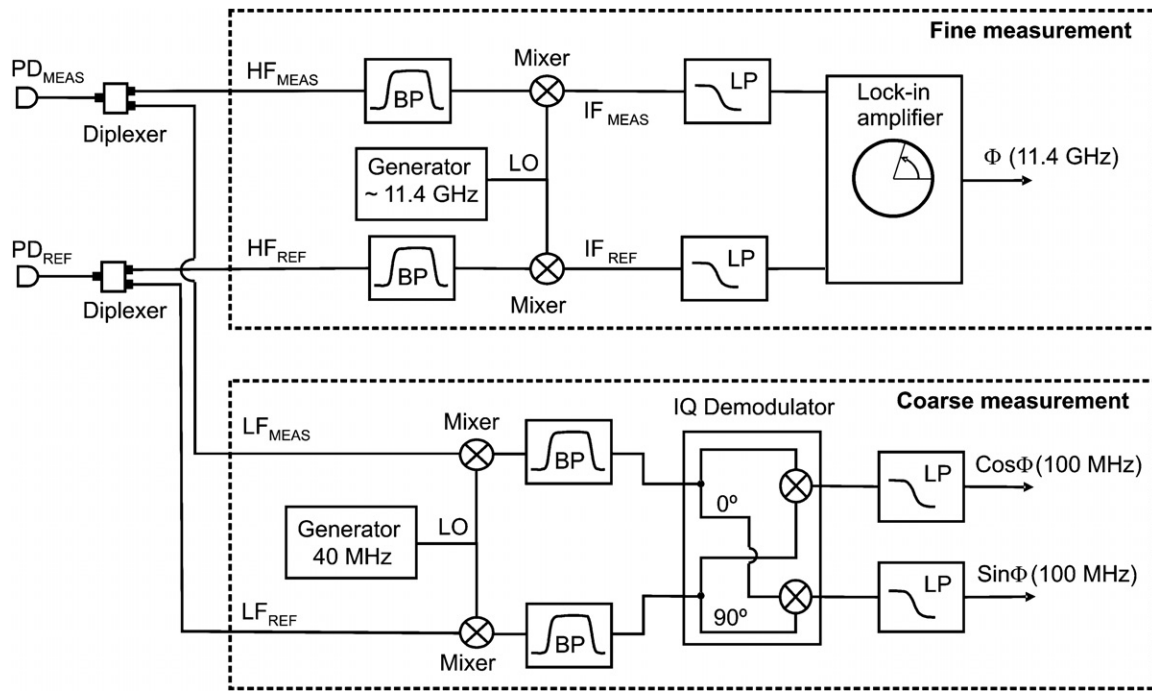


Figure 3. Block diagram of the electronic signal processing to deduce both fine and coarse measurements.

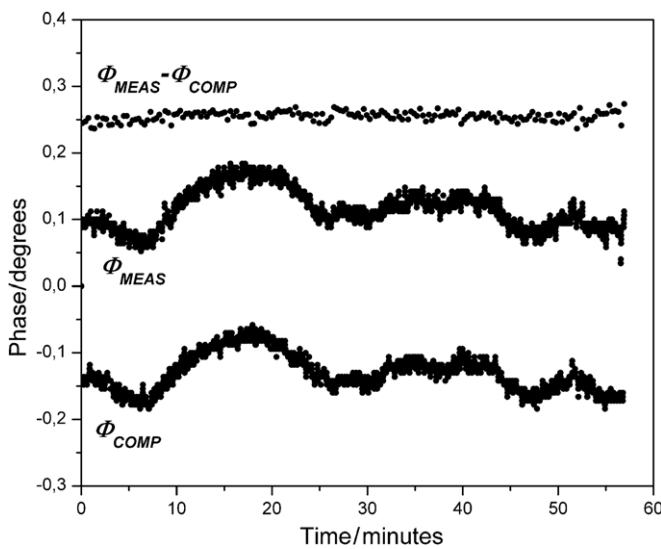


Figure 4. The subtraction of the compensation phase Φ_{COMP} from the measurement phase Φ_{MEAS} cancels out the slow drift effect induced by thermal expansion of the electronic cables.

The lowest frequency comb lines at $f_2 = f_{rep}$ of both measurement and reference signals are mixed with the signal of a second local oscillator (Tektronix AFG 3102, $f = 40$ MHz), generating an intermediary frequency of 60 MHz. The quadrature signals corresponding to the phase of the coarse measurement can then be deduced by an analogue IQ-demodulator (Mini-Circuits MIQ-60WD). The unambiguous range Λ_2 of the coarse measurement amounts to 1.5 m. Compared to using an IQdemodulator working directly at 100 MHz, this configuration has the advantage of enabling the Heydemann correction [19] for the ellipse fit of the quadrature

signals in a static position of the triple-mirror target. The data of the ellipse on the Lissajous diagram are obtained over a large number of 2π periods by using two local oscillator signals with slightly different frequencies. The ellipse fit parameters turned out to be independent of the measurement distance of the target, so that only a single set of fit parameters is necessary for an entire length measurement process. Finally, the phase values are determined from the corrected quadrature signals by the arctangent function.

4. Measurement results and discussion

The system was characterized in the geodetic base of the Physikalisch-Technische Bundesanstalt (PTB). An optical guideway of 50 m length was used and the optical path was extended to 100 m by beam folding. The measurement results were compared to those obtained by the incremental reference HeNe laser interferometer of the PTB.

The experiments presented in this paper were aimed to verify the functionality of the measurement principle, and therefore the fine and the coarse measurements were performed and analysed separately. The data of the reference interferometer were used as input for the unwrapping processes for both the coarse and the fine measurements. The ambient conditions temperature, humidity and pressure were measured by a sensor network and used to correct the index of refraction according to the Edlén equation in the modification by Bönsch and Potulski [18] for both systems, fs-EDM and HeNe reference interferometer. Figure 5 depicts the comparison of the results obtained with the reference HeNe laser system, for both (a) the coarse and (b) the fine measurement steps. As can be seen in figure 5(a), the deviations of the coarse measurement from the reference interferometer data remain within half

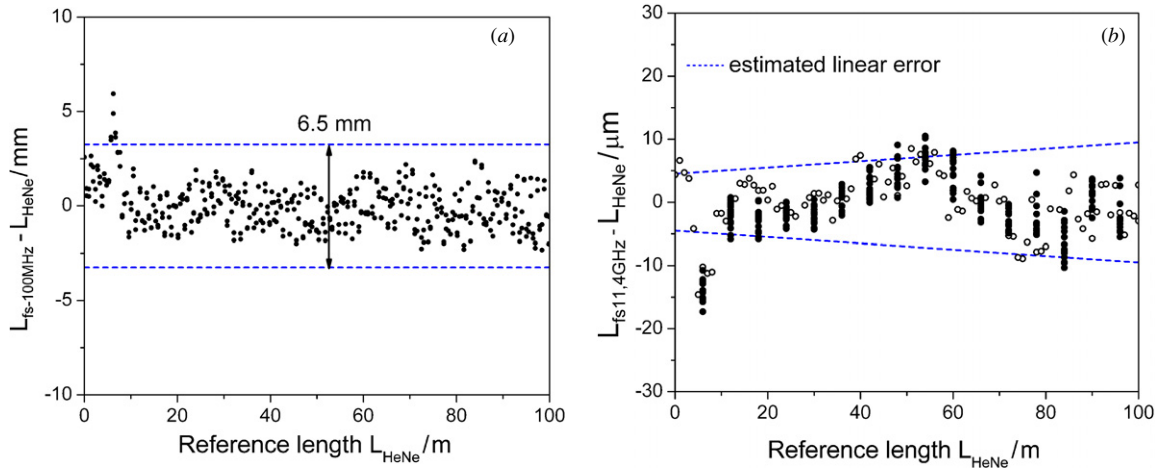


Figure 5. Length difference between the HeNe reference interferometer and the fs distance measurement system: (a) coarse measurement from the 100 MHz signal and (b) fine measurement obtained from the 11.4 GHz signal. The result of the fine determination is depicted over seven measurements with 6 m steps (full symbols), and one measurement with 1 m steps (empty symbols). The integer orders N_1 and N_2 were determined from the reference HeNe signal.

of the unambiguity interval of the fine measurement. The necessary condition for unwrapping the phase data of the f_1 signal is therefore in fact fulfilled, so that the overall measurement uncertainty for the total length is not affected by the measurement uncertainty of the coarse measurement [5].

For the fine measurement, an empirical uncertainty can be graphically estimated from the data depicted in figure 5(b):

$$u_{\text{emp}} = \pm \left(4.5 \mu\text{m} + 0.05 \frac{\mu\text{m}}{\text{m}} \times l \right). \quad (6)$$

The performance of our system reached the level of the work presented in [14], in which measurements up to 200 m showed a similar level of uncertainty, lower than $10 \mu\text{m}$. Nevertheless, in the 100 m range, the deviation from the reference length in our case is only about 50% of the data given in [14].

The uncertainty is hence dominated for shorter distances by a relatively large constant contribution. Assuming that the integer orders N_1 and N_2 have been determined correctly, the uncertainty $u(l)$ can be extracted from equations (2) and (5), resulting in

$$u(l)^2 = \left(\frac{c}{4\pi f_1 n_g} u(\Phi_1) \right)^2 + \left(l \frac{u(f_1)}{f_1} \right)^2 + \left(l \frac{u(n_g)}{n_g} \right)^2. \quad (7)$$

In the following, the individual terms in equation (7) will be discussed in detail. The constant term of the measurement uncertainty is in part attributed to phase instabilities and drifts. The phase detection with the lock-in amplifier is characterized by an uncertainty of 0.02° , corresponding to $u(l)$ of $0.8 \mu\text{m}$. Moreover, the generation of microwave signals in the photodiodes is characterized by excess phase noise via the conversion of amplitude noise to phase noise [20, 21]. In our experiments, the collimation of the measurement laser beam was adjusted so that the maximum signal amplitude occurred when the retroreflector crossed the middle sector of the mechanical guideway. In other words the focus of the backreflected light overlaps with the collimation system

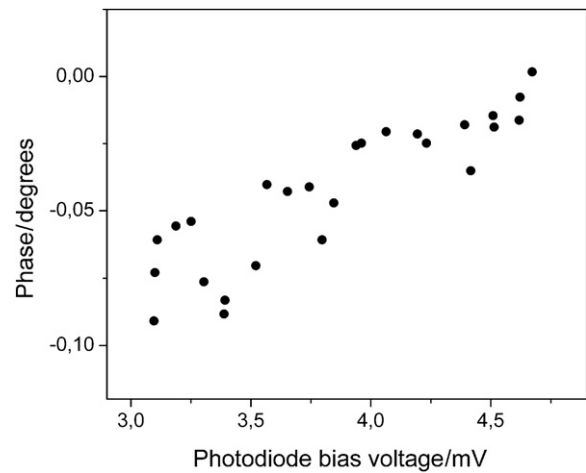


Figure 6. Phase variation of the measurement signal at f_1 with the bias voltage of the photodiode, which is proportional to the intensity of the incident light on the detector.

aperture when the triple-mirror travels over the middle range of the guideway. As a result, there was a variation of about 25% in the signal amplitude, depending on the location of the reflector across the guideway. This effect can be avoided by maintaining the measuring signal constant at each step, using a neutral filter [14]. In addition, the measurement signal amplitude fluctuated by approximately 30% due to air turbulence. Based on these considerations, it is reasonable to assume the amplitude to phase noise conversion effect to be a major contribution to the relatively large constant measurement uncertainty, as well as to the larger deviation from the reference interferometer values in the middle part of the mechanical guideway; see figure 5(b). This effect was studied experimentally. The phase variation of the measurement beam was monitored for a fixed distance of the retroreflector, while the intensity of the beam was sequentially changed using a neutral filter. In figure 6, the observed phase variation is depicted. The data show that

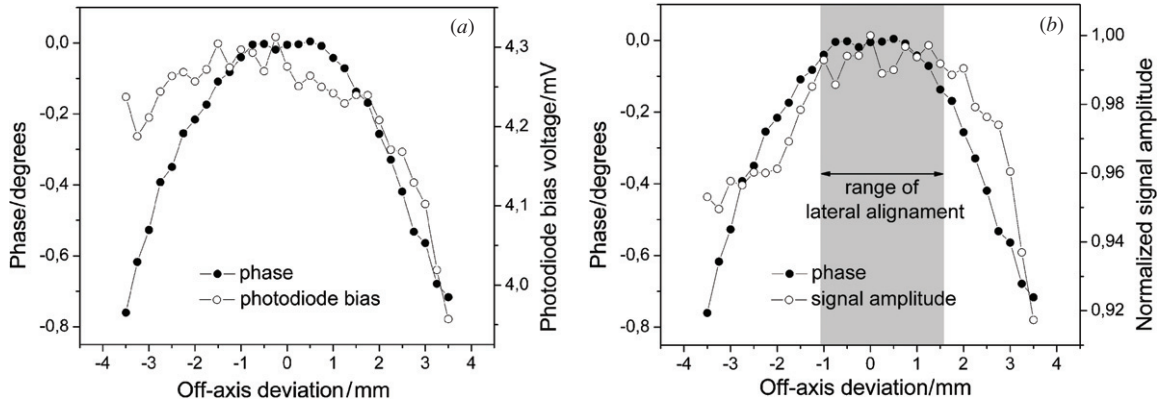


Figure 7. Variation of the measurement signal phase at f_1 (a) of the detector bias voltage dependence and (b) of the signal amplitude with the in-plane off-axis deviation of the retroreflector.

a 30% fluctuation in amplitude implies a phase shift error of 0.1° , corresponding to an uncertainty $u(l)$ of $3.6 \mu\text{m}$

Besides changes in amplitude, changes in the beam position on the photodiode can also induce phase errors [20]. Thus, any off-axis linearity deviation of the guideway can result in changing the focus point of the measurement beam on the detector surface. Therefore, the influence of off-axis deviations of the retroreflector was investigated. Figure 7 shows the phase variation of the measurement signal at frequency f_1 , which occurs by sequentially changing the in-plane offset position of the reflector placed at a fixed distance. In fact, these data provide an explanation for the considerably large deviations from the reference values observed at different positions on the mechanical guideway, e.g. at 6 m or at 84 m, see figure 5(b) for comparison. Although it may seem that the deviation at 6 m is the typical result of the diffraction aperture effect for short distance range, as described in [15], this effect was not observed in our experiments. These unwanted effects appear at the locations where there are unavoidable off-axis linearity deviations (± 2 mm) of the guideway. At these positions, the location of the focus point of the measurement beam changes on the sensitive area of the photodiode PD_{MEAS} , leading to these fluctuation errors. Note that in figure 7 no direct correlation between phase shift error, detector bias and microwave signal variations can be observed. For the length measurements, the adjustment for the detection was optimized by monitoring the maximum of the signal amplitude, not for the detector bias voltage. Based on the data from figure 7(b), over the maximum plateau of the signal amplitude, a phase uncertainty of 0.045° was found, corresponding to $u(l)$ of $0.51 \mu\text{m}$.

The second term of equation (7) adds a length-dependent contribution to the measurement uncertainty. This term is attributed to the relative uncertainty of the pulse repetition rate f_{rep} , where $f_1 = 114 \cdot f_{\text{rep}}$. By testing the repetition rate with a frequency counter, a frequency standard deviation of 1.5×10^{-8} for 3 s integration time was observed, corresponding to a length dependence of $0.015 \mu\text{m m}^{-1}$. Due to the fact that our laser system was referenced to a standard frequency generator, the pulse repetition rate has not reached the stability in which atomic clocks are used as reference.

The third term in equation (7) is determined by the uncertainty of the group refractive index. In the case of our experiments, however, both methods, the fs system and the HeNe laser reference system, use the same correction of the refractive index of air based on the same sensor information. Therefore, uncertainties caused by the determination of the index of refraction do not occur in figure 5 and are not discussed in this context. The measurement uncertainty neglecting contributions from the uncertainty of the index of refraction is hence finally obtained with a coverage factor of $k = 2$ as

$$U(l) = \sqrt{(4.1 \mu\text{m})^2 + (0.02 \mu\text{m m}^{-1})^2 l^2}. \quad (8)$$

The measurement uncertainty is dominated by a relatively large constant term, the length dependence being almost negligible in comparison. This relatively simple technique is hence highly interesting for the measurement of long distances. Nevertheless, we emphasize that the length-dependent uncertainty rises significantly when the influence of the ambient conditions on the index of refraction cannot be neglected, i.e. for actual distance measurements in air. In this case, the implementation of suitable inline compensation schemes (see, e.g., [7, 22]) is necessary to sustain a comparable measurement uncertainty level.

5. Conclusions

In this study, an absolute distance measurement system based on a fs fibre laser source was investigated. A high precision on long distance was achieved by an interpolating measurement approach based on the phase analysis of two distinct frequencies of the microwave comb produced by direct detection of fs laser pulses. The system was verified in an air-conditioned laboratory for distances up to 100 m. The experimental comparison of the fine measurement to a reference counting HeNe interferometer showed deviations smaller than $\pm 10 \mu\text{m}$ at 100 m distance, corresponding to a measurement uncertainty of $1 \times 10^{-7} L$. A thorough analysis of the sources of uncertainty was performed. In the controlled ambient conditions used for this experiment, the observed uncertainty can be mainly attributed to the

conversion of amplitude noise to phase noise and to pointing fluctuation effects which manifest at focusing of the laser beam on the photodetector. Both dominant sources of intrinsic measurement uncertainty are thus dominated by length-independent effects. The presented measurement system will thus be capable of high-precision length measurements of up to 1 km.

Acknowledgments

The authors would like to thank Harald Schnatz for helpful discussions. This research is in part funded by the European Community's Seventh Framework Programme ERA-NET Plus, under grant agreement 217257. The research was performed within the EURAMET joint research project 'Absolute Long-distance Measurement in Air'.

References

- [1] Kim S W 2009 Metrology: combs rule *Nat. Photon.* **3** 313
- [2] Wallerand J P *et al* 2008 Towards new absolute long-distance measurement in air *NCSL Int. Workshop and Symp. (Orlando, USA)* http://www.longdistanceproject.eu/files/towards_new_absolute.pdf
- [3] Hartmann L, Meiners-Hagen K and Abou-Zeid A 2008 An absolute distance interferometer with two external cavity diode lasers *Meas. Sci. Technol.* **19** 045307
- [4] Meiners-Hagen K, Schödel R, Pollinger F and Abou-Zeid A 2009 Multi-wavelength interferometry for length measurements using diode lasers *Meas. Sci. Rev.* **9** 16
- [5] Pollinger F, Meiners-Hagen K, Wedde M and Abou-Zeid A 2009 Diode-laser-based high-precision absolute distance interferometer of 20 m range *Appl. Opt.* **48** 6188
- [6] Salvadé Y, Schuhler N, Lévêque S and Le Floch S 2008 High-accuracy absolute distance measurement using frequency comb referenced multiwavelength source *Appl. Opt.* **47** 2715
- [7] Minoshima K and Matsumoto H 2000 High-accuracy measurement of 240-m distance in an optical tunnel by use of a compact femtosecond laser *Appl. Opt.* **39** 5512
- [8] Joo K N, Kim Y and Kim S W 2008 Distance measurements by combined method based on a femtosecond pulse laser *Opt. Express* **16** 19799
- [9] Balling P, Kren P, Mašika P and van den Berg S A 2009 Femtosecond frequency comb based distance measurement in air *Opt. Express* **17** 9300
- [10] Ye J 2004 Absolute measurement of a long, arbitrary distance to less than an optical fringe *Opt. Lett.* **29** 1153
- [11] Cui M, Zeitouny M G, Bhattacharya N, van den Berg S A, Urbach H P and Braat J J M 2009 High-accuracy long-distance measurements in air with a frequency comb laser *Opt. Lett.* **34** 1982
- [12] Coddington I, Swann W C, Nenadovic L and Newbury N R 2009 Rapid and precise absolute distance measurements at long range *Nat. Photon.* **3** 351
- [13] Matsumoto H, Minoshima K and Telada S 2003 High-precision long-distance measurement using a frequency comb of a femtosecond mode-locked laser *Proc. SPIE* **5190** 308
- [14] Minoshima K, Schibli T R, Matsumoto H, Iino Y, Yoshino K and Kumagai K 2006 Ultrahigh dynamic-range portable distance meter using an optical frequency comb *Conf. on Lasers and Electro-Optics/Quantum Electronics and Laser Science Conf. and Photonic Applications Systems Technologies, Technical Digest (CD) CMYI*
- [15] Minoshima K, Inaba H, Matsumoto H, Iino Y and Kumagai K 2007 Ultrahigh dynamic-range distance measurement using a femtosecond frequency comb *Digest of the IEEE/LEOS Summer Topical Meetings* p 186
- [16] Born M and Wolf E 1991 *Principles of Optics: Electromagnetic Theory of Propagation, Interference and Diffraction of Light* 6th edn (Oxford: Pergamon) p 20
- [17] Ciddor P E and Hill R J 1999 Refractive index of air: 2. Group index *Appl. Opt.* **38** 1667
- [18] Bönsch B and Potulski E 1998 Measurement of the refractive index of air and comparison with modified Edlen's formula *Metrologia* **35** 133
- [19] Heydemann P L M 1981 Determination and correction of quadrature fringe measurement errors in interferometers *Appl. Opt.* **20** 3382
- [20] Ivanov E N, Diddams S A and Hollberg L 2003 Analysis of noise mechanisms limiting the frequency stability of microwave signals generated with a femtosecond laser *IEEE J. Sel. Top. Quantum Electron.* **9** 1059
- [21] Bartels A, Diddams S A, Oates C W, Wilpers G, Bergquist J C, Oskay W H and Hollberg L 2005 Femtosecond-laser-based synthesis of ultrastable microwave signals from optical frequency references *Opt. Lett.* **30** 667
- [22] Meiners-Hagen K and Abou-Zeid A 2008 Refractive index determination in length measurement by two-colour interferometry *Meas. Sci. Technol.* **19** 084004